J. Fluid Mech. (1966), *vol.* 26, *part* 3, *pp.* 515–536

Printed in Great Britain

The boundary-layer regime for convection in a rectangular cavity

By A. E. GILL

Department of Applied Mathematics and Theoretical Physics,
University of Cambridge

(Received 28 January 1966)

This paper studies the two-dimensional convective motion in a rectangular cavity, the two vertical sides of which are maintained at different temperatures. This system is studied for the special case in which the temperature difference ΔT between the two vertical walls is so large that the transfer of heat from one vertical wall to the other is achieved almost entirely by *convection*. Heat transfer by *conduction* is assumed to be of importance only in thin boundary layers adjoining the walls. For a cavity of height H, the boundary layers on the two vertical walls are found to have thickness proportional to ℓ, where $\ell^4 = \kappa\nu H/\gamma g \Delta T$, and the condition for the boundary-layer regime to be established is that ℓ be small compared with the width of the cavity. An approximate solution of the problem is obtained for the case of large values of the Prandtl number ν/κ, and found to be in satisfactory agreement with experimental results obtained by Elder (1965).

1. Introduction

The fact that air is a good insulator has been appreciated and utilized in the construction of buildings for many years. For instance, in the construction of dwellings, it is common practice to build walls consisting of two thicknesses of brick separated by an unventilated air gap of a few inches. Heating engineers have therefore been concerned with discovering how much heat is transferred across the air gap, and with how the rate at which heat is transferred depends on the distance between the two vertical walls and on the temperature difference between them. The problem has been formulated in the following two-dimensional form (Batchelor 1954). A fluid of kinematic viscosity ν, thermal diffusivity κ, and with coefficient of cubical expansion γ, fills a rectangular cavity bounded by two vertical walls, distance L apart, and two horizontal walls, distance H apart. If the two vertical walls are maintained at different temperatures T_a and T_b, at what rate is heat transferred through the fluid from one vertical wall to the other?

The problem has also been of some interest to geophysicists. In many naturally occurring situations, fluid motion results from variations in the buoyancy force which are a consequence of horizontal temperature gradients in the fluid. This fact has led to theoretical and experimental studies of the role played by buoyancy forces in a variety of circumstances. The problem formulated above has been studied for this reason, perhaps because of the simplicity of the geometry rather than because of any direct relevance to a particular geophysical situation. The emphasis of the geophysicist, however, is different from that of the heating engineer. The former is more concerned with details of the motion of the fluid and of the temperature distribution within the fluid rather than with the rate of

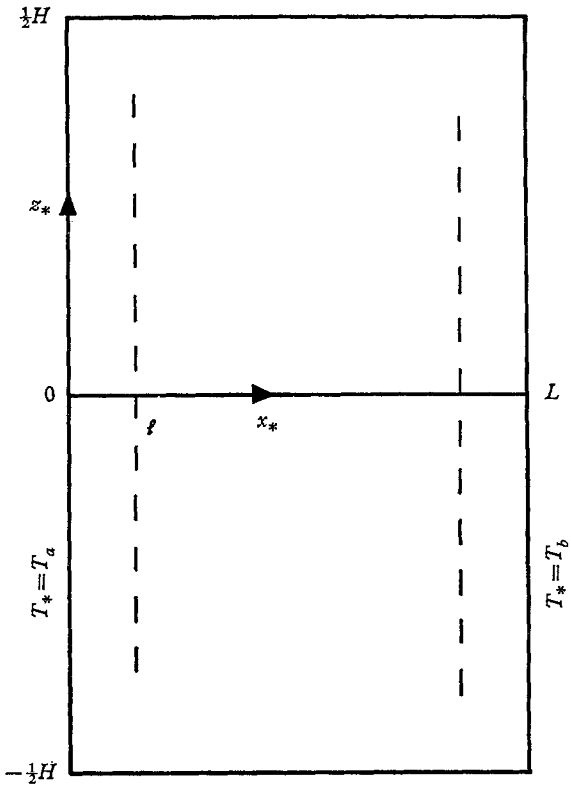

FIGURE 1. The co-ordinate system. The broken lines indicate the extent of the boundary layers.

transfer of heat across the cavity which is the concern of the latter. However, to find the rate of heat transfer, one needs to calculate details of the fluid motion and temperature distribution, so the same calculations are required whatever the emphasis.

The geometry and boundary conditions of the problem are summarized in figure 1. Cartesian co-ordinates (x_*, z_*) have been introduced with origin at the mid-point of the left-hand vertical boundary, and with the z_*-axis directed vertically upwards. The boundary conditions which must be satisfied by the temperature T_* within the fluid are:

(i) That the temperature takes on the imposed values $T_* = T_a$ and $T_* = T_b$ on the two vertical walls, $x_* = 0$ and $x_* = L$ respectively.

(ii) That there is no transfer of heat across the horizontal boundaries; that is, $\partial T_*/\partial z_* = 0$ on $z_* = \pm\frac{1}{2}H$.

The convention is adopted that the left-hand wall is hotter than the right-hand wall, that is, that $T_a > T_b$, so that the temperature difference between the two vertical walls is $\Delta T = T_a - T_b$. The exact condition to be imposed on the temperature field at the two horizontal boundaries $z_* = \pm \frac{1}{2}H$ is not thought to affect the solution a great deal, and the condition (ii) above is only to be regarded as one possibility. In the work to follow, it is assumed, in fact, that a different condition on the temperature field at the two horizontal boundaries would only alter the solution significantly in the immediate vicinity of those boundaries. This assumption will preclude some extreme cases, of course, such as that of very long horizontal boundaries (L/H very large).

Suppose that (u_*, w_*) are the two components of the velocity of the fluid corresponding respectively to the co-ordinates (x_*, z_*). Then the equations to be satisfied by u_*, w_*, T_* are the heat equation

$$u_* \frac{\partial T_*}{\partial x_*} + w_* \frac{\partial T_*}{\partial z_*} = \kappa \left(\frac{\partial^2 T_*}{\partial x_*^2} + \frac{\partial^2 T_*}{\partial z_*^2} \right), \tag{1.1}$$

the continuity equation, which implies the existence of a stream function ψ_*, such that

$$u_* = -\partial\psi_*/\partial z_* \quad \text{and} \quad w_* = \partial\psi_*/\partial x_*, \tag{1.2}$$

and the vorticity equation

$$u_* \frac{\partial \zeta_*}{\partial x_*} + w_* \frac{\partial \zeta_*}{\partial z_*} = \nu \left(\frac{\partial^2 \zeta_*}{\partial x_*^2} + \frac{\partial^2 \zeta_*}{\partial z_*^2} \right) + \gamma g \frac{\partial T_*}{\partial x_*}, \tag{1.3}$$

where

$$\zeta_* = \frac{\partial^2 \psi_*}{\partial x_*^2} + \frac{\partial^2 \psi_*}{\partial z_*^2} \tag{1.4}$$

is the vorticity and g is the acceleration due to gravity. The Boussinesq approximation has been made, namely that density differences due to temperature differences are only of importance in producing differences in the buoyancy force. It has been assumed that the properties ν, κ and γ of the fluid do not change significantly in the temperature range $T_a \leqslant T_* \leqslant T_b$. This assumption is valid if the temperature difference $\Delta T = T_a - T_b$ is sufficiently small, but is often violated in practice because of the rapid variation of kinematic viscosity with temperature. It is thought that the method of approximation used later may be adaptable to include some effects of variation of ν with T_*, but such effects will not be considered here, at least on the grounds that this would introduce another parameter into the problem. The boundary conditions on ψ_* and T_* are

$$\psi_* = \partial\psi_*/\partial x_* = 0, \quad T_* = T_a \quad \text{on} \quad x_* = 0, \tag{1.5}$$

$$\psi_* = \partial\psi_*/\partial x_* = 0, \quad T_* = T_b \quad \text{on} \quad x_* = L, \tag{1.6}$$

and

$$\psi_* = \partial\psi_*/\partial z_* = \partial T_*/\partial z_* = 0 \quad \text{on} \quad z_* = \pm\tfrac{1}{2}H. \tag{1.7}$$

The problem is to find the functions $\psi_*(x_*, z_*)$ and $T_*(x_*, z_*)$ which satisfy the equations (1.1)–(1.4) and boundary conditions (1.5)–(1.7).

The theory of the problem has been considered previously by Batchelor (1954), who pointed out that there are three independent non-dimensional parameters on which the solution depends, as an examination of the equations and boundary conditions shows. One, the aspect ratio H/L, depends only on the geometry of the system and another, the Prandtl number, $\sigma = \nu/\kappa$, is a property of the fluid. The third parameter, involving the imposed temperature difference ΔT, is the Rayleigh number,

$$A = \gamma g \Delta T L^3/\kappa\nu. \tag{1.8}$$

Another property of the equations and boundary conditions is that they are unaltered by a simultaneous change of sign of the three variables, $T_* - \frac{1}{2}(T_a + T_b)$, $x_* - \frac{1}{2}L$ and z_*, while the sign of the fourth variable ψ_* is unchanged. Since this is a symmetry property involving reflexion about the centre $x_* = \frac{1}{2}L$, $z_* = 0$ of the cavity, it is termed the centro-symmetry property of the equations and boundary conditions.

Batchelor showed that for sufficiently small values of the Rayleigh number, that is, for sufficiently small temperature differences ΔT, or sufficiently small distance L between the vertical walls, the transfer of heat from one vertical wall to the other is mainly by conduction. The temperature distribution and flow pattern predicted have since been confirmed in experiments by Eckert & Carlson (1961), Mordchelles-Regnier & Kaplan (1963) and by Elder (1965). These experiments have also confirmed Batchelor's prediction that, for sufficiently large values of the Rayleigh number, the vertical motion is confined mainly to boundary layers on the two vertical walls, and that the transfer of heat from one vertical wall to the other is mainly by convection. However, the core of the cavity, that is, the region not included in any of the boundary layers, is not isothermal as Batchelor suggested, the temperature T_* in the core being found to depend on the vertical co-ordinate z_*. In this paper, attention will be restricted to this boundary-layer regime which is found to exist for sufficiently large values of the Rayleigh number A.

2. The equations and boundary conditions for boundary layers on the vertical walls

Suppose the thickness of the boundary layers on the vertical walls is of order ℓ. It will be assumed that this horizontal length scale ℓ of the boundary layers is small compared with the vertical length scale H, so that an approximation to (1.1)–(1.4) can be made in the boundary layers in the usual way (Goldstein 1938, p. 638). It will also be assumed that the thickness ℓ of the boundary layers is small compared with the width L of the cavity, so that the boundary layers on the two walls are distinct, and separated by a core region.

The orders of magnitude Ψ, ℓ of the stream function and horizontal length in the boundary layers can be deduced from the equations (1.1)–(1.4) in terms of the known orders of magnitude ΔT, H of the temperature and vertical length respectively. First, using the relation (1.2) between velocity components and stream function, it can be seen that the convection terms which comprise the left-hand side of (1.1) are of order $\Psi\Delta T/\ell H$, while the conduction terms on the right-hand side are of order $\kappa\Delta T/\ell^2$. Now, for the case where heat transfer from one vertical wall to the other is mainly by convection, convection terms in (1.1) can be expected to be important in the boundary layer. Also, since heat transfer into the fluid can only be by conduction, these terms must also be important. A balance between conduction and convection requires that

$$\Psi\Delta T/\ell H \sim \kappa\Delta T/\ell^2,$$

i.e.
$$\Psi \sim \kappa H/\ell. \tag{2.1}$$

Similarly, in (1.3), the convection terms on the left-hand side are of order $\Psi^2/\ell^3 H \sim \kappa^2 H/\ell^5$ by (2.1). The diffusion terms on the right-hand side are of order $\nu\Psi/\ell^4 \sim \nu\kappa H/\ell^5$, by (2.1), while the buoyancy term is of order $\gamma g\Delta T/\ell$. The ratio between the diffusion terms and the convection terms is of order $\nu/\kappa = \sigma$, the Prandtl number. If the Prandtl number is large, the diffusion term is large compared with the convection term, and a balance with the buoyancy term which generates the motion gives

$$\nu\kappa H/\ell^5 \sim \gamma g\Delta T/\ell,$$

i.e.
$$\ell^4 \sim \nu\kappa H/(\gamma g\Delta T). \tag{2.2}$$

The same magnitude applies if σ is of order unity, although the convection terms need to be retained. Since, for most fluids other than liquid metals, the Prandtl number is not small, (2.2) will be used to define a horizontal length scale. For small-Prandtl-number fluids, the above scale analysis indicates that convection terms will be more important than diffusion terms over most of the boundary layers, but diffusion terms must be important in a sublayer since these terms contain the highest derivatives. For the moment, both convection and diffusion terms will be retained in the boundary-layer approximation.

The relations (2.1) and (2.2) can now be used to define scales for the stream function and horizontal co-ordinate by replacing $\sim$ by $=$ in these equations. Thus the following non-dimensional variables are defined:

$$\left.\begin{aligned} x = x_*/\ell, \quad z = z_*/H, \quad T = \{T_* - \tfrac{1}{2}(T_A + T_B)\}/\Delta T, \\ \psi = \psi_*/\Psi, \quad u = (H/\Psi)u_*, \quad w = (\ell/\Psi)w_*, \quad \zeta = (\ell^2/\Psi)\zeta_*, \end{aligned}\right\} \tag{2.3}$$

where
$$\ell^4 = \nu\kappa H/(\gamma g\Delta T) \quad \text{and} \quad \Psi = \kappa H/\ell. \tag{2.4}$$

The non-dimensional horizontal co-ordinate x is chosen so that $x = 0$ on the left-hand vertical boundary, and the boundary condition (1.5) becomes

$$\psi = \psi_x = 0, \quad T = \tfrac{1}{2} \quad \text{on} \quad x = 0, \tag{2.5}$$

where the suffix x denotes differentiation with respect to x. The boundary-layer equations, that is the approximate forms of (1.1)–(1.4) valid in the boundary layers, are, in non-dimensional variables,

$$uT_x + wT_z = T_{xx}, \tag{2.6}$$

$$u = -\psi_z, \quad w = \psi_x, \tag{2.7}$$

$$(1/\sigma)(u\zeta_x + w\zeta_z) = \zeta_{xx} + T_x, \tag{2.8}$$

$$\zeta = \psi_{xx} = w_x. \tag{2.9}$$

The boundary conditions for the layer on the left-hand vertical wall are (i) the conditions (2.5) at $x = 0$, (ii) that, as $z \to \pm\frac{1}{2}$, the solution must match solutions valid near $z = \pm\frac{1}{2}$, that is, in the corners, (iii) that, as $x \to \infty$, the solution must match a solution valid in the core.

The boundary condition (iii)

In order for the boundary layers to be distinct, and hence for a core region to exist, it must be assumed that the width ℓ of the boundary layers is small in comparison with the width L of the cavity. Using the definition (2.4) of ℓ, this condition can be written as

$$\left(\frac{L}{\ell}\right)^4 = \frac{\gamma g \Delta T L^4}{\nu\kappa H} = \frac{A}{H/L} \gg 1. \tag{2.10}$$

Note that $(L/\ell)^4$ can be interpreted as a Rayleigh number based on a vertical temperature *gradient* of $\Delta T/H$ and a length L. In terms of the Rayleigh number A, as usually defined (by (1.8)), $(L/\ell)^4$ is equal to the quotient of A and the aspect ratio H/L.

The meaning of the sign $\gg$ in (2.10) has to be interpreted carefully. In a numerical sense, it is found later that L/ℓ needs to be greater than about 12 for the boundary layers to be regarded as at all distinct, which implies that $(L/\ell)^4$ needs to be greater than 2×10^4. Analytically, of course, the meaning is that an approximation to the solution is sought which is valid asymptotically in the limit as $\ell/L \to 0$. Another condition has also to be satisfied by ℓ, namely that, for the boundary-layer equations to be valid, ℓ/H must be small. This condition is satisfied automatically in the limit as $\ell/L \to 0$ if the aspect ratio H/L is kept fixed, but, of course, less restrictive assumptions on the behaviour of H/L as $\ell/L \to 0$ are possible.

The boundary condition (iii) can now be deduced without reference to the dynamical equations. The essential difference between the core and the boundary layer is that the horizontal length scale in the core is much greater than in the boundary layer. In fact one will expect the horizontal length scale in the core to be L, the width of the cavity. For instance, if the scale of the stream function in the core is the same as in the boundary layer, the core solution will have the form

$$\psi = \psi_C\left(\frac{x_*}{L}, \frac{z_*}{H}\right) = \psi_C\left(\frac{\ell}{L}x, z\right).$$

The matching process involves consideration of values of x_* such that, as $\ell/L \to 0$, $x_*/L = (\ell/L)x \to 0$ while $x \to \infty$ (for instance, $x_*/L = (\ell/L)^{\frac{1}{2}}$), thus corresponding to points which remain simultaneously in the core and in the boundary layer. For such values of x_*, the core solution shows that, as $\ell/L \to 0$,

$$\psi \to \psi_C(0, z) = \psi_0(z), \text{ say.} \tag{2.11}$$

This, therefore, is a condition on the boundary-layer solution to be satisfied as $x \to \infty$, provided that the scale of the stream function is the same in the core as in the boundary layer. If, on the other hand, changes in the stream function in the core are small compared with those in the boundary layer, the corresponding condition on the boundary-layer solution is $\psi \to$ const. as $x \to \infty$, which may be regarded as a special case of (2.11).

There remains a further possibility, namely that the volume flux in the core is large compared with that in the boundary layer. This alternative will not be considered here on the grounds that *experiments* clearly show that this is not the case. However, no reason seems to have been found for rejecting this possibility on *theoretical* grounds. In fact, Batchelor (1954, § 6) has built up a seemingly consistent picture in which the boundary condition corresponding to (2.11) is that w tends to a function of z as $x \to \infty$. The core is also assumed to be isothermal. Weinbaum (1964) used such a model for convection in a horizontal circular cylinder, although experiments of Martini & Churchill (1960) show that when such a cylinder is heated from the side there is, contrary to Weinbaum's assumptions, more volume flux in the boundary layer than in the core, and the temperature in the core does vary with the vertical co-ordinate z. This is a special case of Weinbaum's, however, in which Weinbaum's own analysis indicates a breakdown of the assumptions on which it was based (Weinbaum 1964, p. 434).

The boundary condition for the temperature in the boundary layer is less ambiguous since the temperature differences in the core cannot be greater than the imposed temperature difference, ΔT. The above reasoning therefore shows that the appropriate boundary condition is

$$T \to T_0(z) \quad \text{as} \quad x \to \infty, \tag{2.12}$$

where T_0 is some function of z.

3. Asymptotic behaviour of the boundary-layer solutions

The boundary-layer equations (2.6)–(2.9) are non-linear, and therefore difficult to treat analytically. However, a great deal of useful information can be derived from a consideration of the asymptotic behaviour of the boundary-layer solutions as $x \to \infty$. This analysis will apply to circumstances in which the boundary conditions (2.11) and (2.12) are applicable, so let

$$T = T_0(z) + \theta(x, z), \tag{3.1}$$

$$\psi = \psi_0(z) + \phi(x, z), \tag{3.2}$$

where (θ, ϕ) represents a perturbation on the solution at $x = \infty$, and so satisfies the conditions

$$\theta, \phi \to 0 \quad \text{as} \quad x \to \infty. \tag{3.3}$$

Before substituting (3.1) and (3.2) in the boundary-layer equations, it may be noted that (2.8) can be integrated with respect to x to give, using (2.9),

$$(1/\sigma)(uw_x + ww_z) = w_{xx} + T - T_0(z), \tag{3.4}$$

where the additive function of z that arises from the integration has been determined from the boundary conditions (2.11) and (2.12). (3.4) is the boundary-layer approximation to the vertical momentum equation.

If now (3.1) and (3.2) are substituted in (2.6), (2.7) and (3.4), and the analysis is restricted to values of x sufficiently large for terms of the second order in (θ, ϕ) to be neglected, the following equations result:

$$u_0(z)\theta_x + T_0'(z)w = \theta_{xx}, \tag{3.5}$$

$$(1/\sigma)u_0(z)w_x = w_{xx} + \theta, \tag{3.6}$$

where

$$u_0(z) = -\psi_0'(z) \tag{3.7}$$

is the horizontal velocity at the outer edge of the boundary layer,

$$w = \psi_x = \phi_x, \tag{3.8}$$

and the prime denotes differentiation with respect to z.

The two equations (3.5), (3.6) involve no derivatives with respect to z, so that z appears in them only as a parameter. They make up a linear system of the fourth order in x, and the coefficients are independent of x, so the solution may be written as a sum of exponentials

$$w = \sum_{n=1}^{4} a_n(z) \exp(-\lambda_n(z)x), \tag{3.9}$$

where $\lambda_n(z)$ are the roots of the quartic equation

$$\lambda^2(\lambda+u_0)\{\lambda+(1/\sigma)u_0\}+T_0' = 0, \tag{3.10}$$

as follows from substitution of (3.9) in the equations. In general, the roots are complex, and so may be written

$$\lambda = \lambda_r + i\lambda_i,$$

where λ_r and λ_i are the real and imaginary parts respectively. The boundary conditions (3.3) require that only terms involving roots with positive λ_r should occur in (3.9). The values of λ_r concerned are important as they determine the rate of decay of θ and ϕ as $x \to \infty$, and so give an indication of the boundary-layer thickness. If the corresponding values of λ_i are non-zero, an oscillatory behaviour of the solutions is indicated.

The behaviour of the roots λ in (3.10) depends on the sign of T_0', so the three cases T_0' zero, negative and positive will be considered in turn.

(*a*) $T_0' = 0$. This corresponds to constant temperature at the outer edge of the boundary layer. An example is the boundary layer on a heated vertical plate in isothermal surroundings (Goldstein 1938, p. 638). The four roots in this case are

$$\lambda = 0, \quad 0, \quad -u_0 \quad \text{and} \quad -(1/\sigma)u_0.$$

It is immediately apparent that a boundary layer can only exist if $u_0 < 0$, that is if the layer *entrains* fluid. The reason is clear from (3.5). When $T_0' = 0$, there is nothing to balance the outward diffusion of heat save horizontal convection, and a balance can only be achieved if the convection is into the layer. This is the case for the boundary layer on a heated vertical plate which entrains fluid at all levels. It is interesting to note that, if the rates of diffusion of heat and momentum differ greatly, that is, if the Prandtl number is substantially different from unity, the two roots $-u_0$ and $-(1/\sigma)u_0$ are very different, and so there are two different boundary-layer thicknesses. For σ large, for instance, there is a relatively thin thermal boundary layer. The differences in buoyancy force which drive the flow are confined to this layer. In it, convection of momentum is weak compared with the very strong diffusion of momentum, with the result that the vertical velocity outside the layer does not vanish, but falls to zero in a much thicker layer outside. This behaviour is shown in computed solutions of the Goldstein problem (Ostrach 1953).

(*b*) $T_0' < 0$. This corresponds to an *unstable* temperature gradient at the outer edge of the boundary layer, and so is hardly likely to occur in practice. Since, by (3.10), the product of the roots is T_0', which is negative, it follows that three roots have real part of one sign and one root has real part of the opposite sign. It turns out that the three roots with real part of the same sign are positive if the layer is entraining and negative if the layer is ejecting. If u_0 is zero, two roots have zero real part.

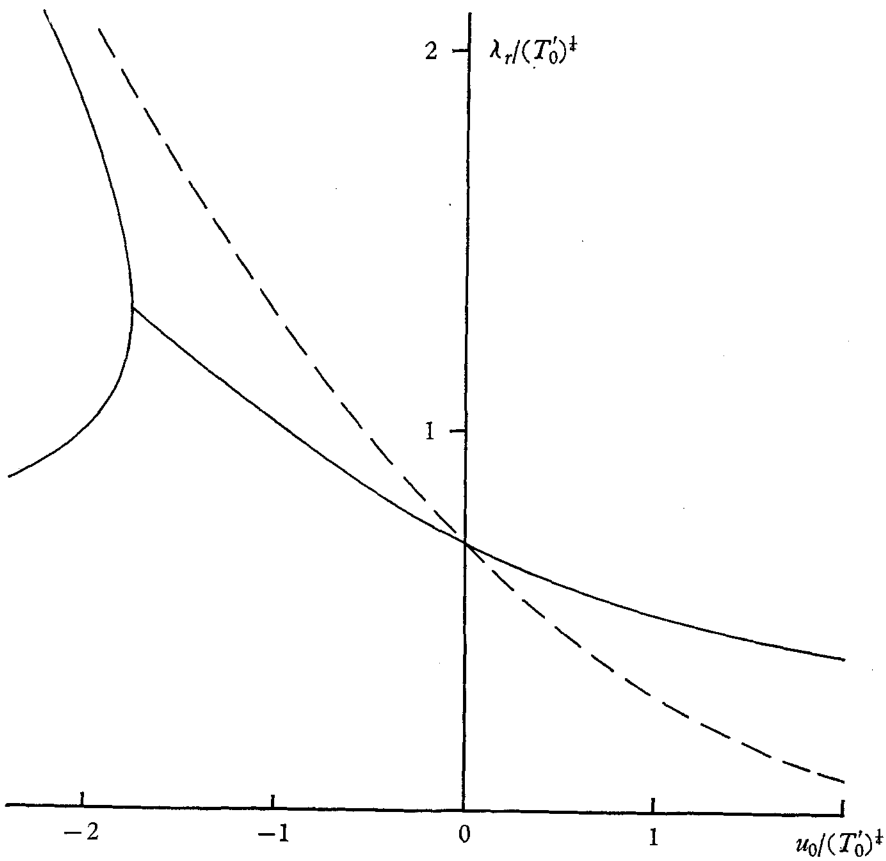

FIGURE 2. The real parts λ_r of the roots λ of the quartic, $\lambda^2(\lambda+u_0)(\lambda+u_0/\sigma)+T_0' = 0$, for $\sigma = 1$ (broken line) and $\sigma = \infty$ (solid line). T_0' is positive, and only positive λ_r are shown. The roots are complex where a single value is shown and real where two are shown. The boundary-layer thickness is proportional to $1/\lambda_r$.

(*c*) $T_0' > 0$. This corresponds to a *stable* temperature gradient at the outer edge of the boundary layer. This is the case of most interest here, since experiments show that there is a stable temperature gradient in the core of a rectangular cavity under the circumstances considered in this paper. An exact solution of the governing equations exists when T_0' is constant, and this is given as an example in the next section. In the case where T_0' is positive, the product of the roots of the equation (3.10) is positive, and it follows that the real parts λ_r of the roots are either all of one sign or that there are two λ_r's of each sign. The fact that the sum of the products of the roots three at a time is zero, by (3.10), eliminates the first possibility. Thus there are two roots with positive real part as required whatever the value of u_0. Thus a stable temperature gradient can support a boundary layer whether it is ejecting or entraining or even if u_0 is zero. In the latter case, the roots are given by

$$(4/T_0')^{\frac{1}{4}}\lambda = \pm 1 \pm i, \tag{3.11}$$

and do not depend on the Prandtl number.

In general, (3.10) shows that $\lambda/(T_0')^{\frac{1}{4}}$ is a function of $u_0/(T_0')^{\frac{1}{4}}$ and σ. Figure 2 shows the positive values of $\lambda_r/(T_0')^{\frac{1}{4}}$ as a function of $u_0/(T_0')^{\frac{1}{4}}$ for the two cases, $\sigma = 1$ and $\sigma = \infty$. If $u_0/(T_0')^{\frac{1}{4}}$ is small, the boundary layer may be said to be controlled by the temperature gradient, and so the two positive values of λ_r are close together and vary little with σ. If, on the other hand, $u_0/(T_0')^{\frac{1}{4}}$ is large, the effect of the temperature gradient is weak, so that, if σ is radically different from one, the two positive values of λ_r become widely separated as in case (*a*).

A physical argument that indicates why a stable temperature gradient can support both entraining ($u_0 < 0$) and ejecting ($u_0 > 0$) layers, in contradistinction to the case $T_0' = 0$, is as follows. Consider a fluid particle in the boundary layer on, say, the hotter wall, and suppose that it is gaining heat by conduction. This gain of heat must be reflected by movement of the particle to a warmer part of the fluid. If there is no vertical temperature gradient, this will generally mean movement toward the wall ($u < 0$). But, if a stable temperature gradient exists, upward movement will carry the particle to a warmer region and so it need *not* move toward the wall.

4. An exact solution of the equations for free convection

There exists an exact solution of the equations (1.1)–(1.4) which admirably illustrates case (*c*) discussed in § 3 above. Furthermore, the approximate analysis of §§ 6 and 7 indicates that this solution is a good approximation to the solution of the cavity problem near $z = 0$, so that it is worth discussing in some detail. It is a special case of a solution given by Prandtl (1952, p. 422) for the 'mountain and valley winds in stratified air', or katabatic winds, the special case being that of a vertical rather than a slanting boundary. It is a solution corresponding to the following situation. An infinite vertical plate is held in a fluid whose temperature at $x_* = \infty$ varies uniformly with height, the uniform temperature gradient G being positive. The temperature of the plate is held at a value which differs by a constant amount, B, from the temperature at infinity. Thus, choosing the origin to be on the plate at the level at which the temperature at infinity is zero, the boundary conditions on the temperature field are

$$T_* = Gz_* \quad \text{at} \quad x_* = \infty$$

and

$$T_* = B + Gz_* \quad \text{at} \quad x_* = 0.$$

A solution exists of the following simple form

$$T_* = \Theta(x_*) + Gz_*, \tag{4.1}$$

$$w = w_*(x_*), \tag{4.2}$$

the boundary conditions on Θ, w_* being

$$\Theta = B, \quad w_* = 0 \quad \text{at} \quad x_* = 0; \tag{4.3}$$

$$\Theta = 0, \quad w_* = 0 \quad \text{at} \quad x_* = \infty. \tag{4.4}$$

Because of the simple form (4.1), (4.2) of the solution, the equations are greatly simplified. The motion is vertical everywhere so there is no horizontal convection and there is no vertical diffusion of momentum. In addition, the vertical temperature gradient has the same value everywhere, so there is no gain of heat at any point due to vertical conduction of heat. Thus the rate of gain of heat of a material particle moving upwards through a vertical temperature gradient G is equal to the rate of gain of heat of the particle due to horizontal conduction of heat; that is, the heat equation is

$$Gw_* = \kappa(d^2\Theta/dx_*^2). \tag{4.5}$$

This equation may be derived by substitution of (4.1), (4.2) in (1.1). The momentum equation is equally simple. The sum of the rate of gain of a vertical momentum of a particle due to horizontal diffusion and the buoyancy force on the particle, relative to that at $x_* = \infty$, is zero, that is

$$0 = \nu(d^2w_*/dx_*^2) + \gamma g\Theta. \tag{4.6}$$

This equation may be derived by substitution of (4.1), (4.2) in (1.2)–(1.4) and integrating once with respect to x_*.

The two equations (4.5), (4.6) combine to give

$$\{\nu\kappa(d^4/dx_*^4) + \gamma gG\}(\Theta, w_*) = 0. \tag{4.7}$$

The horizontal length scale ℓ involved is given by

$$\ell^4 = 4\nu\kappa/(\gamma gG), \tag{4.8}$$

which corresponds to (2.4) if the temperature gradient $\Delta T/H$ is identified with $\frac{1}{4}G$. The factor 4 is included for convenience. The solution of (4.5), (4.6) satisfying (4.3), (4.4) is

$$\Theta = B\,e^{-x}\cos x, \tag{4.9}$$

$$w_* = (\gamma g\kappa/\nu G)^{\frac{1}{2}} B\,e^{-x}\sin x, \tag{4.10}$$

where $x = x_*/\ell$ as in (2.3). It is interesting to note that equations (4.5), (4.6) are the same as equations (3.5), (3.6) when $u_0 \equiv 0$ and $T_0' \equiv$ const. Hence, when there is no entrainment and the temperature gradient is constant, the asymptotic solution is valid everywhere.

Four noteworthy features of the solution (4.9), (4.10) are that:

1. there is no dependence on the Prandtl number;
2. the vertical velocity is independent of height and there is no entrainment;
3. there is a change in sign of the vertical velocity at $x = \pi$, and a weak reverse flow for $\pi < x < 2\pi$. The same oscillating behaviour is shown by the temperature, which, at a fixed level, overshoots its asymptotic value to reach a maximum (or minimum) at $x = \frac{1}{2}\pi$;
4. the boundary layer has constant thickness ℓ.

As $G \to 0$, the thickness ℓ of the layer tends to infinity. This is consistent with the result for a *semi*-infinite plate for $G = 0$ (Goldstein 1938, p. 638), which gives a boundary-layer thickness that grows indefinitely with distance along the plate. A stable temperature gradient G may therefore be regarded as limiting the thickness of the boundary layer in the same way that rotation can limit the thickness of an ordinary boundary layer. The above solution is in fact analogous to the solution for an Ekman layer (see, for example, Prandtl 1952, p. 356), due to the well-known analogy between the motions of rotating and of stratified fluids (an example is given by Jeffreys 1928, § 7). The analogy may be useful when considering the stability of the flow (4.9), (4.10) to small disturbances, as this will be related to the stability of an Ekman layer. For time-dependent flows of real fluids, the analogy works only when heat and momentum diffuse at the same rate, that is only for unit Prandtl number. Given this, the equations satisfied by u_*, $\Theta = T_* - Gz_*$, and w_* are the same as those for the velocity components u_*, v_*, w_* relative to a frame rotating with angular velocity Ω about the x_* axis, provided they depend only on x_*, z_* and time t_*. Ω can be identified with ν/ℓ^2 where ℓ is given by (4.8) and v_* identified with $-(\gamma g/G)^{\frac{1}{2}}\Theta$.

5. The core solution

After the general discussion of the last two paragraphs, let us return to the cavity problem and consider the solution in the core. It will be assumed (see discussion at end of § 2) that the scales of the stream function, temperature and vertical distance are the same as those in the boundary layer, that is Ψ, ΔT and H respectively. Ψ is defined by (2.4). Taking the horizontal length as the width L of the cavity, the orders of magnitude of the various terms in (1.1)–(1.4) can be compared with the aid of the conditions $\ell \ll H$ and $\ell \ll L$. It will be assumed that the Prandtl number σ is either large or of order unity.

The relative order of the various terms in (1.1), (1.3) will depend on the aspect ratio, H/L. In (1.3), the convection and diffusion terms are respectively of orders $\ell^2/\sigma(L^2+H^2)$ and $\ell^3L/(L^2+H^2)^2$ compared with the buoyancy term. These orders of magnitude are both small compared with unity provided $L \ll H^4/\ell^3$, so if this condition is satisfied (1.3) reduces in the core to

$$\partial T_*/\partial x_* = 0.$$

Thus the core solution is, in non-dimensional terms,

$$T = T_0(z), \tag{5.1}$$

where $T_0(z)$ is the same function as that which occurs in (2.12).

In (1.1), the conduction terms are of order $\ell L/(L^2+H^2)$ relative to the convection terms, and this order of magnitude is small compared with unity provided

$$L \ll H^2/\ell, \tag{5.2}$$

and if this condition is satisfied so is the condition $L \ll H^4/\ell^3 = (H^2/\ell)(H^2/\ell^2)$ required for (5.1) to be valid. In that case the heat equation reduces in the core to

$$T_0'(z)\,\partial\psi_*/\partial x_* = 0. \tag{5.3}$$

If T_0' were zero, the temperature scale in the core would not be ΔT as assumed, so this equation implies that in the core

$$\psi = \psi_0(z), \tag{5.4}$$

where ψ_0 is the same function as that in (2.11).

It will be assumed that (5.2) holds so that (5.1) and (5.4) are valid first approximations in the core. The condition (5.2) can only be violated if the aspect ratio H/L is small, that is, for a cavity whose height is much smaller than its width. The neglected term of highest order is the vertical conduction term in the heat equation (1.1). So, to the next level of approximation,

$$\psi = \psi_0(z) + \frac{\ell L}{H^2}\left[\left(\frac{x_*}{L} - \frac{1}{2}\right)\frac{T_0''(z)}{T_0'(z)} + \psi_1(z)\right], \tag{5.5}$$

where ψ_1 is some function of z. Thus the small slope of the streamlines is given in terms of first-order quantities by

$$\frac{w_*}{u_*} = -\frac{\partial\psi_*/\partial x_*}{\partial\psi_*/\partial z_*} = \frac{\ell}{H}\frac{T_0''(z)}{u_0(z)\,T_0'(z)}. \tag{5.6}$$

Because of the centro-symmetry property mentioned in § 1, T_0 must be an odd and ψ_0 an even function of z. In particular $u_0(0) = -\psi_0'(0) = 0$ and the solutions of (3.10) at $z = 0$ are given by (3.11). This solution does not depend on the Prandtl number so it may be concluded that the solution near $z = 0$ depends very little on the Prandtl number.

6. An approximate solution to the convection problem

In order to find an approximate solution to the convection problem, it is first necessary to find an approximate solution to the boundary-layer equations, (2.6) and (3.4). The method employed for this purpose follows a modification of the Oseen technique suggested by Carrier (1962). It is based here on the observation that, at each level $z =$ const., the quantities u and T_z appearing in the convection terms vary across the boundary layers from zero on the vertical boundaries to values of $u_0(z)$ and $T_0'(z)$, respectively, in the core. As an approximation, u and T_z will be replaced at each level, $z =$ const., by average values $u_A(z)$ and $T_A'(z)$ which will presumably lie between zero and the core values $u_0(z)$ and $T_0'(z)$, respectively. By symmetry, u_A will be an odd and T_A' an even function of z.

In the subsequent analysis, the case of infinite Prandtl number, $\sigma = \infty$, is chosen. In Elder's (1965) experiments σ was large, of order 1000. (3.4) then becomes a linear equation as the left-hand side vanishes. Thus it is only necessary to approximate the heat equation (2.6). When the average values are substituted it becomes

$$u_A(z)T_x + T_A'(z)w = T_{xx},$$

or, using (3.1),

$$u_A(z)\theta_x + T_A'(z)w = \theta_{xx}. \tag{6.1}$$

Similarly, for $\sigma = \infty$, (3.4) becomes

$$0 = w_{xx} + \theta. \tag{6.2}$$

These equations have the same form as (3.5), (3.6) when $\sigma = \infty$, the only difference being that the suffix A replaces the suffix 0. Thus the solution has the form (3.9) where λ_n are now the roots of

$$\lambda^3(\lambda + u_A(z)) + T_A'(z) = 0. \tag{6.3}$$

Figure 2 shows the positive values of $\lambda_r/(T_A')^{\frac{1}{4}}$ as functions of $u_A/(T_A')^{\frac{1}{4}}$.

Since the solutions are now approximate solutions for the whole of the boundary layer, the boundary conditions (2.5) may be applied. Thus

$$w = \frac{\frac{1}{2}-T_0}{\lambda_2^2-\lambda_1^2}(-e^{-\lambda_2 x}+e^{-\lambda_1 x}), \tag{6.4}$$

$$\theta = \frac{\frac{1}{2}-T_0}{\lambda_2^2-\lambda_1^2}(\lambda_2^2 e^{-\lambda_2 x}-\lambda_1^2 e^{-\lambda_1 x}), \tag{6.5}$$

where λ_1, λ_2 are the roots with positive real part of (6.3).

To relate the average values of u_A, T'_A to the core values u_0, T'_0, integral conditions can be used following Karman and Pohlhausen (cf. Goldstein 1938, p. 641). Suitable integrals are the conservation of mass and heat, integrals with respect to x of (2.7) and (2.6) respectively. They are

$$\psi_0(z) = \int_0^\infty w\,dx, \tag{6.6}$$

$$\frac{d}{dz}\int_0^\infty w\theta\,dx+\psi_0(z)\,T'_0(z) = -(\theta_x)_{x=0}. \tag{6.7}$$

Momentum is conserved automatically since (3.4) is satisfied exactly.

Substituting (6.4), (6.5) in (6.6), (6.7) gives

$$\psi_0 = \frac{\frac{1}{2}-T_0}{\lambda_1\lambda_2(\lambda_1+\lambda_2)}, \tag{6.8}$$

$$\frac{d}{dz}\left(\frac{(\frac{1}{2}-T_0)^2}{2(\lambda_1+\lambda_2)^2}\right)+\psi_0 T'_0 = (\tfrac{1}{2}-T_0)\left(\lambda_1+\lambda_2-\frac{\lambda_1\lambda_2}{\lambda_1+\lambda_2}\right), \tag{6.9}$$

where λ_1, λ_2 are the roots with positive real part of (6.3). Since the integrals do not depend on which root is called λ_1 and which λ_2, they only involve the invariants

$$\tau = \lambda_1+\lambda_2 \quad\text{and}\quad \chi = \lambda_1\lambda_2, \tag{6.10}$$

and these invariants are related to u_A and T'_A by (6.3). The relationship is relatively simple because of the fact that u_A and T_A are odd functions of z. Thus (6.3) is invariant under the transformation $z\to -z$, $\lambda\to-\lambda$ and so the four roots are $\lambda_1(z)$, $\lambda_2(z)$, $-\lambda_1(-z)$ and $-\lambda_2(-z)$. Comparing (6.3) with

$$(\lambda-\lambda_1(z))\,(\lambda-\lambda_2(z))\,(\lambda+\lambda_1(-z))\,(\lambda+\lambda_2(-z)) = 0,$$

and equating like powers of λ gives

$$\left.\begin{aligned} \tau(-z)-\tau(z) &= u_A, \\ \chi(z)+\chi(-z) &= \tau(z)\,\tau(-z), \\ \tau(z)\,\chi(-z) &= \tau(-z)\,\chi(z), \\ \chi(z)\,\chi(-z) &= T'_A. \end{aligned}\right\} \tag{6.11}$$

Elimination of $\tau(-z)$ and $\chi(-z)$ would lead to the required relations.

In addition to the two equations (6.8), (6.9) relating the four unknown functions u_0, T_0, u_A, and T_A, two similar ones may be obtained by applying the integrals to the other boundary layer, giving four equations in all. Four equivalent equations may be obtained by taking odd and even parts of (6.8), (6.9), using the property that u_0, T_0, u_A and T_A are all odd functions of z. To make full use of this symmetry property, the invariants τ and χ will be expressed in terms of odd and even functions, q and v. The even function is defined by

$$v = \tau(-z)+\tau(z). \tag{6.12}$$

Instead of using $u_A = \tau(-z)-\tau(z)$ as the odd function, it is convenient to define

$$q = u_A/v. \tag{6.13}$$

Then using (6.10)–(6.13), τ, χ and λ may be expressed in terms of the odd function q and the even function v.

$$\left.\begin{aligned} \tau &= \tfrac{1}{2}v(1-q), \\ \chi &= \tfrac{1}{8}v^2(1-q^2)(1-q), \\ \lambda_{1,2} &= \tfrac{1}{4}v(1-q)[1\pm i\sqrt{(1+2q)}]. \end{aligned}\right\} \tag{6.14}$$

q, in fact, gives a measure of the parameter

$$\frac{u_A}{(T'_A)^{\frac{1}{4}}} = \frac{q}{(\frac{1}{4}(1-q^2))^{\frac{3}{4}}}, \tag{6.15}$$

and varies between ± 1. For $|q| < \frac{1}{2}$, the roots are complex, and the boundary layer is controlled mainly by the temperature gradient (§ 3 (c)) for q small. For $q < -\frac{1}{2}$, the roots are real and become widely separated as $q \to -1$, so that the boundary layer has a double structure (§ 3 (a)). $q > \frac{1}{2}$ represents an ejecting layer weakly controlled by the temperature gradient (§ 3 (c)).

The solution of (6.8), (6.9) involves some algebra, and only the main steps will be outlined. First, (6.14) may be used to substitute for $\tau = \lambda_1+\lambda_2$ and $\chi = \lambda_1\lambda_2$ in (6.8), (6.9). The odd and even parts of the resulting equations then make up four equations relating ψ_0, T_0, q and v. The odd and even parts of (6.8) give

$$\left.\begin{aligned} \psi_0 &= \frac{8}{v^3(1-q^4)}, \\ T_0 &= \frac{q}{1+q^2}. \end{aligned}\right\} \tag{6.16}$$

These expressions may be substituted in (6.9), the odd and even parts of which give two differential equations involving q, v, and their derivatives with respect to z. The quotient of the two equations gives dv/dq as a function of q and v, and integrates to give

$$v = \frac{2(1+3q^2)^{\frac{11}{9}}}{C(1+q^2)^{\frac{2}{3}}(1-q^2)}, \tag{6.17}$$

where C is a constant. Comparing this equation with (6.16), ψ_0 is found as a function of q,

$$\psi_0 = C^3(1+q^2)(1-q^2)^2(1+3q^2)^{-\frac{11}{3}}. \tag{6.18}$$

It remains to find q as a function of z. This can be done by substituting (6.17) in the odd part of (6.9) to give

$$\frac{dz}{dq} = \frac{C^4(7-q^2)(1-q^2)^3(1+q^2)^{\frac{2}{3}}}{2(1+3q^2)^{\frac{53}{9}}}. \tag{6.19}$$

If the integration is started from $z = 0$, where $q = 0$, the integral contains only one unknown, the value C^3 of ψ_0 at $z = 0$. Equation (6.19) shows that C occurs only in a scale factor for z. This scale factor could be determined by matching the core solution with solutions valid in boundary layers on the horizontal boundaries. These boundary layers will be thin and, in the limit as their thickness tends to zero, one might expect that the full boundary conditions (1.7) could be replaced by a condition on the core solution.

The appropriate condition to apply would seem to be that the boundary layer has emptied itself by the time it reaches the top, that is, that

$$\psi_0 = 0 \quad \text{at} \quad z = \pm\tfrac{1}{2}. \tag{6.20}$$

This condition is equivalent to requiring that, in the boundary layers on the vertical walls, $w = 0$ at $z = \pm\frac{1}{2}$, and (6.4) shows this requires $T_0 = \frac{1}{2}$ or $\lambda_{1,2} = \infty$. In fact it is found that $T_0 = \frac{1}{2}$ at $z = \frac{1}{2}$ and $\lambda_{1,2} = \infty$ at $z = -\frac{1}{2}$. The former condition corresponds to all the fluid having been warmed to a temperature $T = \frac{1}{2}$ by the time it reaches the top of the warm wall. This warm fluid is carried across the top of the core. Correspondingly, cold fluid at temperature $T = -\frac{1}{2}$ enters the boundary layer at the bottom of the warm wall, while the temperature on the wall itself is $T = +\frac{1}{2}$. Thus there is a singularity at the bottom of the warm wall, as there is also in the Goldstein solution at the bottom of an isolated warm wall.

7. Results

The results obtained by integrating (6.19) and so finding T_0, ψ_0, etc. as functions of z are shown in figures 3–7. For the results shown in figures 4–7, the scaling factor C^4 in (6.19) has been chosen so that the condition (6.20) is satisfied. This condition gives the value $C^4 = 0{\cdot}693$, and leaves *no disposable constants*. For figure 3, C has been chosen differently as described below. Let us now consider each figure in turn.

Figure 3 shows the temperature T_0 in the core as a function of vertical position z. The plotted points are experimental values taken from Elder (1965, figure 4 (*b*)). The solid line is the theoretical curve, scaled with a value of C chosen to give the same gradient at the point where $T_0 = 0$ as in the experiments, and positioned so that $T_0 = 0$ at the same place as in the experiments. Discrepancies between theory and experiment should then show up as differences in the shapes of the curves, and, in particular, in the positions at which $T_0 = \pm 0{\cdot}5$. The curves agree well in the lower half of the cavity, but not so well in the upper half. This fact points to the *asymmetry* in the experimental curves, in contradistinction to the symmetry predicted from the equations and boundary conditions discussed in this paper. The main reason for the asymmetry in the experiments is thought to be the variation of viscosity with temperature. For instance, the viscosity of the silicone oil used by Elder varies by a factor of 3 over the largest temperature range (35·5 °C) quoted in Elder's table 1. This seems a very large factor, but the viscosity appears in the theory only to the one-quarter power, and $\nu^{\frac{1}{4}}$ will only vary $\pm 15\,\%$ from its mean value if ν varies by a factor of 3.

Note that the theory gives a temperature gradient that approaches infinity as $z \to \pm 0{\cdot}5$. In practice the gradient will be limited by diffusion and the curve will be modified in the boundary layers on the horizontal boundaries.

The boundary-layer thickness $1/\lambda_r$ can be found from (6.14) once q is found as a function of z. The variation of this thickness with vertical position is shown in figure 4(*a*). Its thickness half-way up is $1{\cdot}8\ell$, where ℓ is given by (2.4).

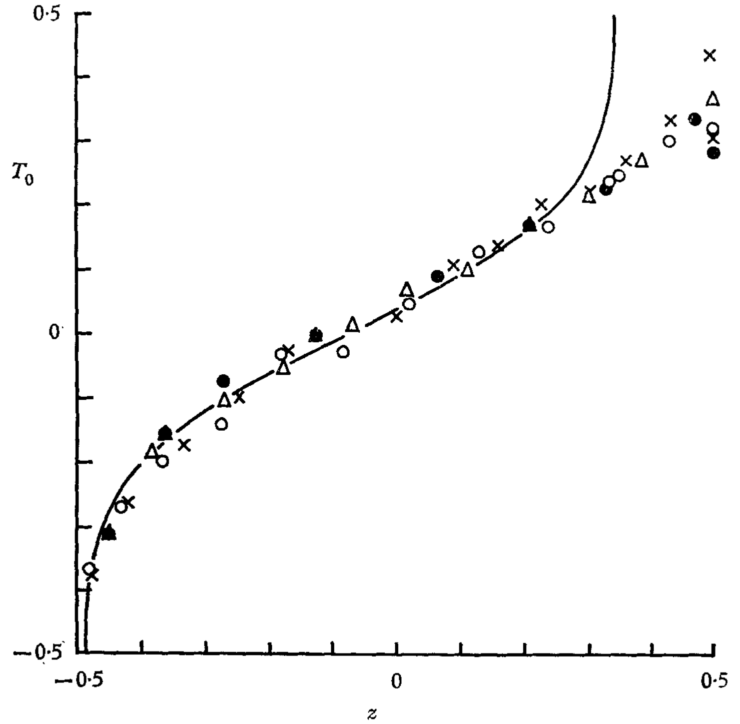

FIGURE 3. The temperature $T_0(z)$ in the core. The solid line is the theoretical curve. The experimental points (Elder 1965, figure 4(*b*)) are for a Rayleigh number of $A = 1{\cdot}2 \times 10^6$ and various aspect ratios, $h = H/L$. $\bigcirc$, $h = 18{\cdot}8$; $\times$, $h = 10{\cdot}0$; $\triangle$, $h = 5{\cdot}0$; $\bullet$, $h = 2{\cdot}5$.

The value ψ_0 of the stream function in the core varies with z as shown in figure 4(*b*). It gives a measure of the mass flux in the boundary layer at each level. The value of the dimensional stream function at the centre of the cavity is $0{\cdot}76\kappa H/\ell$, where ℓ is given by (2.4). The gradient of ψ_0, $\psi_0' = -u_0$, is a measure of the horizontal velocity in the core. The theory gives $u_0 \to \infty$ as $z \to \pm 0{\cdot}5$, but in practice diffusion will limit u_0 to a finite value and the solution will be modified in thin layers near the top and bottom. Note that most of the flux across the core takes place near the upper and lower boundaries.

In figure 4(*c*), the variation with z of the local Nusselt number $(-\theta_x)_{x=0}$ is depicted. The value half-way up is $0{\cdot}27$.

When T_0, λ_1 and λ_2 have been found as functions of z using (6.14), (6.16), (6.19) and C has been chosen to satisfy (6.20), the variations of vertical velocity w and temperature θ in the boundary layer can be found from (6.4), (6.5), at least to the approximation of the theory. The values given by the theory at any point are uniquely determined since there are no disposable constants. At $z = 0$, the solution has the same form as the exact solution (4.9), (4.10), essentially because the entrainment is zero there.

In figure 5, the variations of temperature with horizontal position are shown for three different levels, and compared with experiment (Elder 1965, figure 3).

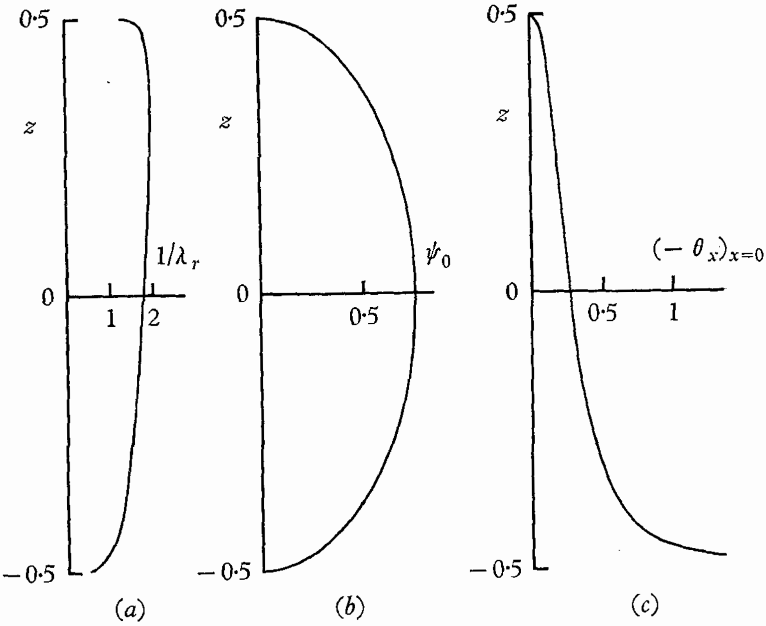

FIGURE 4. (*a*) The boundary-layer thickness $1/\lambda_r$, (*b*) the stream function ψ_0 for the core, and (*c*) the local Nusselt number, $(-\theta_x)_{x=0}$, as functions of z.

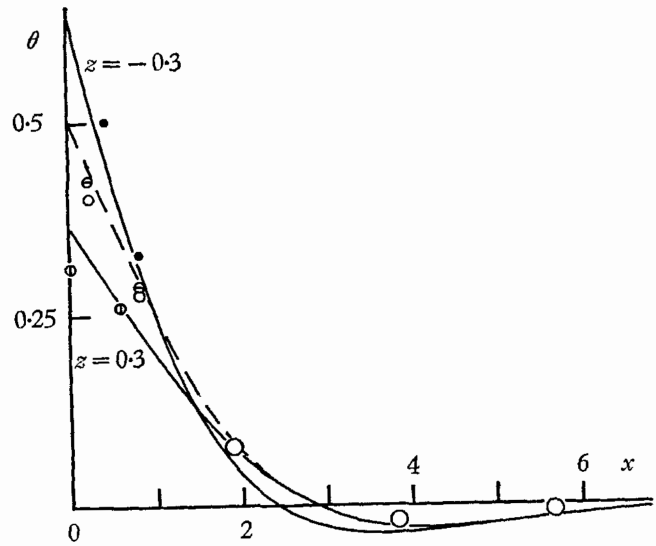

FIGURE 5. The horizontal variation of the temperature, $\theta = T - T_0$, at the levels $z = 0$, $\pm 0{\cdot}3$. The broken line corresponds to $z = 0$. The experimental points are from Elder 1965, figure 3, and correspond to the levels indicated. ●, $z = -0{\cdot}3$; ⊖, $z = -0{\cdot}1$; ○, $z = 0{\cdot}1$; ⦶, $z = 0{\cdot}3$; ◯, all 4 preceding values.

The agreement is very good, considering that there are no arbitrary constants available for curve fitting. The curve for $z = 0$ has the same form as (4.9).

Similarly, in figure 6 good agrement is found for velocity profiles $w(x)$ at different levels, comparison being made with Elder's figure 7. The velocity scale was determined using the value $\kappa = 1{\cdot}05 \times 10^{-3}\,\text{cm}^2\,\text{sec}^{-1}$ appropriate to the silicone oil used in the experiments. The curve for $z = 0$ has the same form as (4.8).

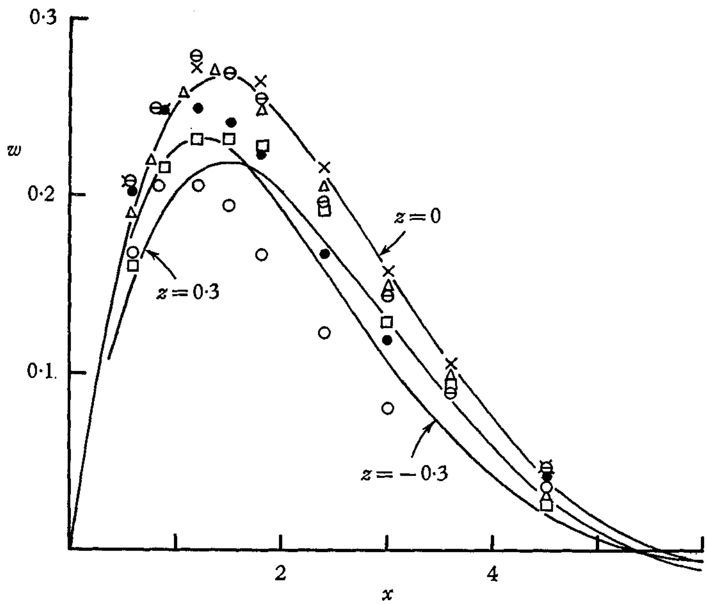

FIGURE 6. The variation of vertical velocity w with horizontal distance x at three different levels, $z = 0, \pm 0{\cdot}3$. The experimental points are from Elder 1965, figure 7, and correspond to the levels indicated. ○, $z = -0{\cdot}37$; ●, $z = -0{\cdot}24$; ⊖, $z = -0{\cdot}10$; ×, $z = 0{\cdot}03$; △, $z = 0{\cdot}16$; □, $z = 0{\cdot}29$.

Further comparison of velocity profiles can be made using Elder's figure 6, which shows $w(x)$ at $z = 0$ for a series of values of $A/(H/L) = (L/\ell)^4$. His theoretical curves are of the same form as given by the above theory at $z = 0$, that is of the same form as (4.10), but he chooses velocity amplitudes which give the best fit with experimental curves. Also his horizontal length scale was slightly smaller (8 %) than that given by the above theory. The comparison is interesting as it gives an indication of how small ℓ/L must be for the boundary-layer theory to be valid. Consider the value of $11{\cdot}5\ell/L$, which is the ratio of the boundary-layer thickness, as measured by the position of the first zero of $w(x)$, to the half-width $\frac{1}{2}L$ of the cavity. For Elder's examples the values are (*a*) 1·8, (*b*) 0·9, (*c*) 0·8 and (*d*) 0·4. The fitted amplitudes are respectively the following fractions of the theoretical values: (*a*) 0·4, (*b*) 0·7, (*c*) 0·8 and (*d*) 1·0. The agreement improves as ℓ/L decreases, but the discrepancy is very large when $11{\cdot}5\ell/L < 1$, that is, when

$$\frac{A}{H/L} = \frac{\gamma g L^4 \Delta T}{\nu\kappa H} > 2\times 10^4.$$

This may be regarded as a condition for the boundary-layer theory to be valid.

The isotherms shown in figure 7(a) were calculated using (6.5). Comparison with Elder's figure 2 shows qualitative agreement except in the boundary layer on the upper surface, which was free in Elder's experiment. For quantitative comparison, note that $x = 4$ corresponds to $x_* = 0{\cdot}34L$ in the experiment. An interesting feature is the reversal of horizontal temperature gradient in the layer which is a feature, for instance, of the exact solution discussed in § 4.

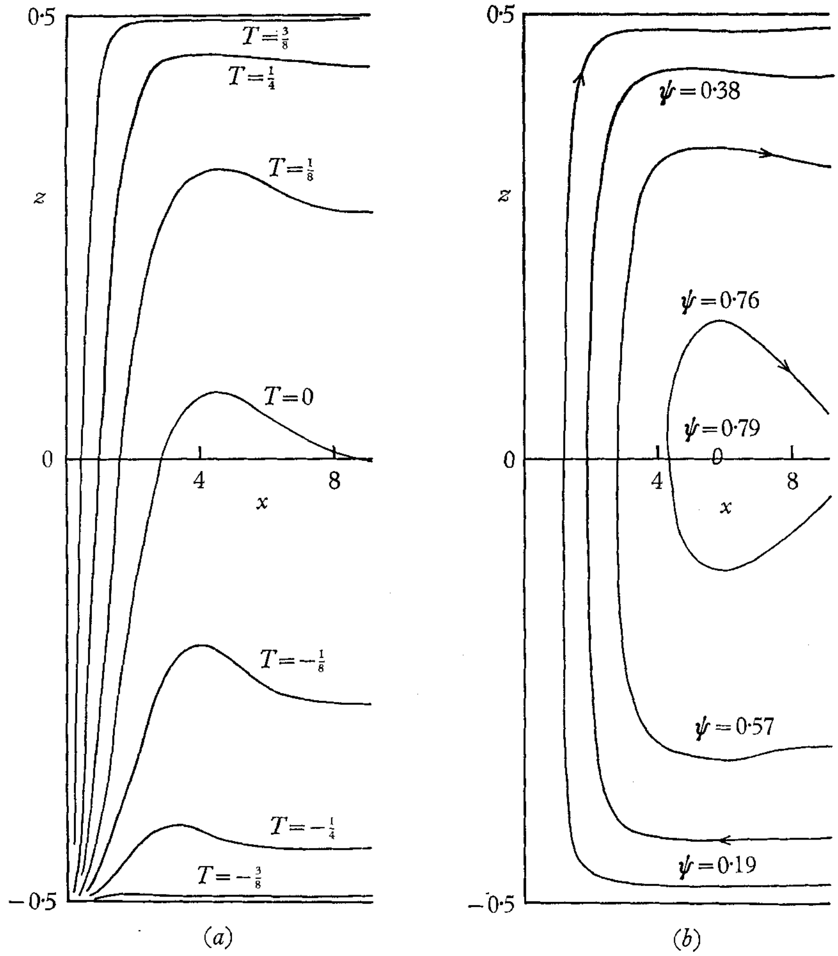

FIGURE 7. (a) Isotherms, and (b) streamlines for the boundary layer on the hot wall. The streamlines are drawn at intervals equal to one quarter of the value of the stream function at the centre of the cavity.

The stream function $\psi(x, z)$ for the boundary layer can be calculated by integration of (6.4) with respect to x. The streamlines are shown in figure 7(b). If the stream function is scaled to 100 at the centre, the streamlines drawn correspond to values of 25, 50, 75 and 100, with a maximum value of 104. Comparison may be made with Elder's figure 8, which shows the same qualitative features. For quantitative comparison, note that $x = 4$ corresponds to $x_* = 0{\cdot}07L$ in the experiment. An interesting feature is the set of closed streamlines in, or partially in, the boundary layer. The experiments show more asymmetry about $z = 0$ than the theory. This could be a second-order feature, as is the small slope of the streamlines, which is of the same order as given by (5.6).

A further feature of the approximate solution, not shown in the figures, is the variation of the parameter q with z. q is a parameter which measures the relative importance of the vertical temperature gradient and the horizontal motion in controlling the dynamics of the boundary layer. Except in the end one-tenth of the cavity, $q < 0{\cdot}3$, so, by (6.15), $u_A/(T'_A)^{\frac{1}{4}} < 1$, implying that, in most of the cavity, the boundary layer is controlled by the vertical temperature gradient. This has the further implication that the flow has only a weak dependence on the Prandtl number, as is indicated by the extreme case of the exact solution discussed in § 4, which does not depend on the Prandtl number at all.

8. Discussion

Neither the boundary layer nor the core solution depend on the Rayleigh number A or the aspect ratio H/L. In the approximate solution found above, these parameters determine only the ratio of the thicknesses of the two regions, which is proportional to $\{(H/L)/A\}^{\frac{1}{4}}$. Effects neglected above which will lead to a slight dependence on A and H/L are:

(i) The small slope of the streamlines. This will lead to solutions that depend on the distance between the two boundary layers;

(ii) the effect of the boundary layers on the horizontal boundaries.

In order to gain a physical insight into the situation, it is perhaps useful to look at it this way. Consider a cavity which is initially at a uniform temperature with one vertical wall held at a higher temperature and the opposite wall at a lower temperature. Boundary layers will begin to form on the vertical boundaries. In the absence of the top and the opposite wall, the boundary layer on the warmer wall would develop into one like the steady boundary layer on an isolated wall (Goldstein 1938, p. 638). This layer entrains fluid at all levels, with the strongest entrainment at the bottom where the horizontal temperature gradients, which are responsible for the flow, are greatest. In the cavity, however, there are two layers competing for fluid, so one would expect the layer on the warmer wall to entrain fluid from the lower half of the cavity, and the layer on the cooler wall to entrain fluid from the upper half.

In the final steady state, there is the same competition for fluid. The entrainment into the lower part of the warmer layer brings fluid from the cooler layer opposite. This influx of cooler fluid maintains a strong horizontal temperature gradient across the layer, and this gradient maintains the upward flow in the layer and the entrainment into the layer. The flow across the core brings cooler fluid into the lower half and warmer fluid into the upper half, leading to a stable vertical temperature gradient in the core. This vertical gradient is of profound importance as it is the main factor in determining the structure of the boundary layers on the vertical wall. Its existence allows the boundary layers to eject as well as to entrain fluid.

The flow in the core is weaker than in the boundary layers on the vertical walls and is not strong enough to maintain a horizontal temperature gradient. Thus the isotherms in the core are horizontal. Since the streamlines in the core tend to follow the isotherms, they are also horizontal in the core.

Finally, viscous and thermal diffusion in the neighbourhood of the horizontal boundaries will tend to limit the velocity and temperature gradients there.

I should like to acknowledge helpful discussions with Dr J. W. Elder. Part of the manuscript was written while visiting the Institute of Geophysics and Planetary Physics of the University of California at San Diego, with support from the National Science Foundation under contract NSF-G-13575.

REFERENCES

BATCHELOR, G. K. 1954 *Quart. J. Appl. Maths.* **12**, 209.

CARRIER, G. F. 1962 *Proc. 10th Int. Conf. Appl. Mech.* Elsevier Publishing Company.

ECKERT, E. R. G. & CARLSON, W. O. 1961 *Int. J. Heat & Mass Trans.* **2**, 106.

ELDER, J. W. 1965 *J. Fluid Mech.* **23**, 77.

GOLDSTEIN, S. 1938 *Modern Developments in Fluid Mechanics.* Oxford: Clarendon Press.

JEFFREYS, H. 1928 *Proc. Roy. Soc.* A **118**, 195.

MARTINI, W. R. & CHURCHILL, S. W. 1960 *A.I.Ch.E.* **6**, 251.

MORDCHELLES-REGNIER, G. & KAPLAN, C. 1963 *Proc. Int. Heat and Mass Transfer Conf.* 94. *Am. Soc. Mech. Eng.*

OSTRACH, S. 1953 *NACA Rep.* no. 1111.

PRANDTL, L. 1952 *Essentials of Fluid Dynamics.* New York: Hafner Publishing Company.

WEINBAUM, S. 1964 *J. Fluid Mech.* **18**, 409.